Dipole Moments, Polarizabilities and the Fluorescence Behaviour of 4-(9-anthryl)-N,N-dimethylaniline

Wolfram Baumann, F. Petzke, and K.-D. Loosen
Institut für physikalische Chemie, Universität Mainz

Z. Naturforsch. **34a**, 1070–1082 (1979); received July 2, 1979

It is shown that the solvent dependence of the fluorescence wavenumber and decay time as well as the solvent dependent effect of an external electric field on the absorption and fluorescence spectra of 4-(9-anthryl)-N,N-dimethylaniline can be fully understood taking into account reaction field induced polarizability effects.

I. Introduction

Electrooptical emission measurements (EOEM) have proved to be a reliable method to determine electric dipole moments of molecules in solutions in excited fluorescent states [1, 2]. As has been pointed out in [1, 3], EOEM give dipole moments of molecules in excited equilibrium states in contrast to electrooptical absorption measurements (EOAM) [4, 5], that give dipole moments of molecules in excited Franck-Condon (FC) states. Equilibrium state means that all nuclei of the solute itself and the surrounding solvent molecules have relaxed after excitation to a new equilibrium before fluorescence takes place. This is valid if the relaxation processes involved are much faster than the fluorescence process. If there is a considerable structural change of the molecule while relaxing from an excited FC to an equilibrium state, one could hope to find different values for the dipole moments of a polar molecule in excited FC and corresponding equilibrium states.

So it seemed to be an interesting experiment to do EOEM work on 4-(9-anthryl)-N,N-dimethylaniline (ADMA) in different solvents, as there are some hints coming from various experiments in the literature that there is a structural change after excitation depending on the solvent used.

Mataga [6, 7, 8, 9] and Chandross [10], too, have found an unusual behaviour of the fluorescence of ADMA. The fluorescence spectrum gets more and more an unstructured and broad band when passing from nonpolar to polar solvents. At the same time the fluorescence is strongly shifted to the red, so indicating a large dipole moment of the fluorescent state. Figure 1 shows a plot of the wavenumber $\tilde{\nu}_e$ of the fluorescence maximum against

$$g = \frac{\varepsilon - 1}{2\varepsilon + 1}$$

for various solvents, where ε is the dielectric constant of the solvent. Mataga's [7] wavenumbers have been used, and the solvent parameter

$$\frac{\varepsilon - 1}{2\varepsilon + 1} - \frac{1}{2} \cdot \frac{n^2 - 1}{2n^2 + 1}$$

as used in Mataga's plot, has been transformed to

$$\frac{\varepsilon - 1}{2\varepsilon + 1} \text{ by setting } \frac{1}{2} \cdot \frac{n^2 - 1}{2n^2 + 1} = 0.1 .$$

This can be done in a very good approximation, because

$$\frac{1}{2} \frac{n^2 - 1}{2n^2 + 1}$$

is nearly not solvent dependent compared with $(\varepsilon - 1)/(2\varepsilon + 1)$.

Obviously, this plot Fig. 1 does not show a straight line. Mataga [7] pointed out that the

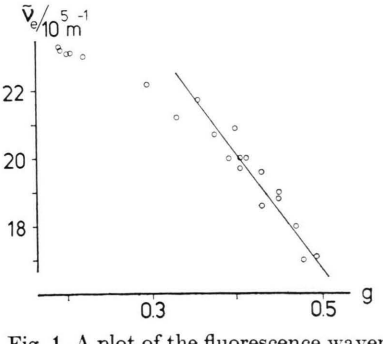

Fig. 1. A plot of the fluorescence wavenumber maximum $\tilde{\nu}_e$ of ADMA against $g = (\varepsilon - 1)/(2\varepsilon + 1)$ as recalculated from Mataga [7] (see text).

Reprint requests to Prof. Dr. W. Baumann, Institut für physikalische Chemie der Universität, Jakob-Welder-Weg 26, D-6500 Mainz.

0340-4811 / 79 / 0900-1070 $ 01.00/0

curvature could be due to a solvent dependent change in the electronic structure of ADMA, resulting in a solvent dependent dipole moment μ_a of the fluorescent species.

Mataga's [6—11] and Grabowski's [12, 13, 14] groups have done much work in order to elucidate the nature of the observed fluorescence.

It seems that all this spectroscopic and kinetic work cannot unambiguously favour a simple model or theory. First of all it is not quite clear whether there are two emitting states or species that have different dipole moments or not. This could be elucidated very simply by electrooptical emission measurements.

Second, even in nonpolar solvents the broad fluorescence band is nearly unstructured, whereas the first absorption band is clearly structured, very similar to 9-phenylanthracene. This is shown in Figure 2.

So, at the first glance it seems that the emitting state could be another possibly structurally relaxed state than that reached by absorption. Time resolved fluorescence and kinetic studies from Grabowski's group [12, 13] seem to show this, although solvent reorientation kinetics could account for the results of these experiments, too [15, 16]. With reference to Fig. 2 it must be emphasized that there is a longwavelength shoulder in the absorption spectrum in contrast to 9-phenylanthracene. Figure 3 shows that this shoulder is redshifted if the solvent polarity is increased.

This shoulder is described by Mataga [7] as a CT transition, possibly of an ADMA conformer. Electrooptical absorption measurements are a very

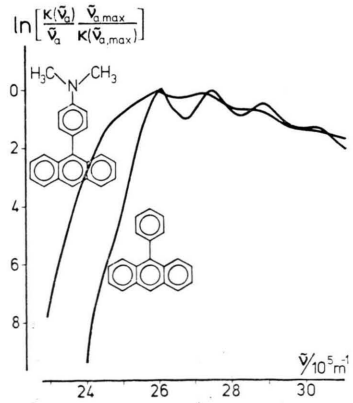

Fig. 2. Absorption spectra of ADMA and 9-phenylanthracene in heptane at 298 K.

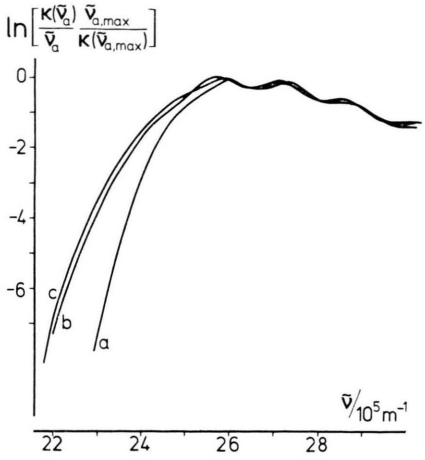

Fig. 3. Solvent dependence of the longwavelength shoulder in the absorption spectrum of ADMA at 298 K. a = heptane, b = dioxane, c = benzotrifluoride.

powerful method to show whether this shoulder is a longwavelength electronic transition to a state more polar than the locally excited state reached by the anthracene-like absorption. The comparison of the dipole moments found in the longwavelength shoulder and in the anthracene-like absorption with the dipole moment determined by electrooptical emission measurements should give a hint to a possible correspondence between the fluorescent state(s) and the FC states reached by absorption.

II. Theoretical and Experimental

The theory for EOEM has been discussed in detail in [3]. EOAM has been developed in a lot of papers by Labhart [17—19] and Liptay [4, 5, 20—23] whose most elaborated theoretical model has been taken for EOEM in [3], too, in order to get results from both methods, which can be compared on the basis of the same model. According to Onsager [24] and Scholte [25] in this model the solute molecule is considered to be a polarizable point dipole fixed in the center of a cavity, the dimensions of which are of the order of the dimensions of the solute. In the most simple case this cavity is approximated by a sphere with radius a. This spherical approximation is used throughout this paper.

If the lifetime of the excited solute molecule is much longer than the orientation relaxation times of the solvent molecules and the solute molecule in

solution, the following equations hold for EOEM [3]:

$$X(\varphi, \tilde{\nu}_e) = A^{e\prime}(\varphi) + B^e(\varphi)\, T^e(\tilde{\nu}_e) + C^e(\varphi)\, U^e(\tilde{\nu}_e) \quad (1)$$

with

$$A^{e\prime}(\varphi) = \frac{D^e}{3} + (3\cos^2\varphi - 1)\frac{E^e + 2D^e}{30} + L(\chi^0, \tilde{\nu}_a{}^0), \quad (2)$$

$$B^e(\varphi) = (2 - \cos^2\varphi)\, F^e + (3\cos^2\varphi - 1)\, G^e, \quad (3)$$

$$C^e(\varphi) = (2 - \cos^2\varphi)\, H^e + (3\cos^2\varphi - 1)\, I^e, \quad (4)$$

$$T^e(\tilde{\nu}_e) = \frac{1}{5hc}\cdot\frac{\mathrm{d}}{\mathrm{d}\tilde{\nu}_e}\ln\frac{p(\tilde{\nu}_e)}{\tilde{\nu}_e{}^3}, \quad (5)$$

$$U^e(\tilde{\nu}_e) = \frac{1}{10h^2c^2}\left[\left(\frac{d}{\mathrm{d}\tilde{\nu}_e}\ln\frac{p(\tilde{\nu}_e)}{\tilde{\nu}_e{}^3}\right)^2 + \frac{\mathrm{d}^2}{\mathrm{d}\tilde{\nu}_e{}^2}\ln\frac{p(\tilde{\nu}_e)}{\tilde{\nu}_e{}^3}\right], \quad (6)$$

where $p(\tilde{\nu}_e)$ is the photon current density emitted at wavenumber $\tilde{\nu}_e$.

$$D^e = 2\beta\,\mathrm{Re}\{\boldsymbol{m}_e\,\mathrm{m}_e{}'\,\boldsymbol{\mu}_a\} + |\,\mathrm{tr}\,\mathrm{m}_e{}'|^2, \quad (7)$$

$$E^e = \beta^2[3(\boldsymbol{m}_e\,\boldsymbol{\mu}_a)^2 - \mu_a{}^2] + \beta(3\,\boldsymbol{m}_e\,\boldsymbol{\alpha}_a\,\boldsymbol{m}_e - \mathrm{tr}\,\boldsymbol{\alpha}_a) + 6\beta\,\mathrm{Re}\{\boldsymbol{m}_e\,\boldsymbol{\mu}_a\cdot\mathrm{tr}\,\mathrm{m}_e{}' + \boldsymbol{\mu}_a\,\mathrm{m}_e{}'\,\boldsymbol{m}_e\} + 6\,|\,\mathrm{tr}\,\mathrm{m}_e{}'|^2, \quad (8)$$

$$F^e = \beta\,\boldsymbol{\mu}_a\,\Delta^e\boldsymbol{\mu} + \tfrac{1}{2}\,\mathrm{tr}\,\Delta^e\boldsymbol{\alpha} + 2\,\mathrm{Re}\{\boldsymbol{m}_e\,\mathrm{m}_e{}'\,\Delta^e\boldsymbol{\mu}\}, \quad (9)$$

$$G^e = \beta(\boldsymbol{m}_e\,\boldsymbol{\mu}_a)(\boldsymbol{m}_e\,\Delta^e\boldsymbol{\mu}) + \tfrac{1}{2}\,\boldsymbol{m}_e\,\Delta^e\boldsymbol{\alpha}\,\boldsymbol{m}_e + \mathrm{Re}\{\boldsymbol{m}_e\,\Delta^e\boldsymbol{\mu}\cdot\mathrm{tr}\,\mathrm{m}_e{}' + \Delta^e\boldsymbol{\mu}\,\mathrm{m}_e{}'\,\boldsymbol{m}_e\}, \quad (10)$$

$$H^e = |\,\Delta^e\boldsymbol{\mu}\,|^2, \quad (11)$$

$$I^e = |\,\boldsymbol{m}_e\,\Delta^e\boldsymbol{\mu}\,|^2. \quad (12)$$

Quite similar equations hold for EOAM [4, 5]:

$$L(\chi, \tilde{\nu}_a) = A^a(\chi) + B^a(\chi)\cdot T^a(\tilde{\nu}_a) + C^a(\chi)\cdot U^a(\tilde{\nu}_a) \quad (13)$$

with

$$A^a(\chi) = \frac{D^a}{3} + (3\cos^2\chi - 1)\frac{E^a + 2D^a}{30}, \quad (14)$$

$$B^a(\chi) = (2 - \cos^2\chi)\, F^a + (3\cos^2\chi - 1)\, G^a, \quad (15)$$

$$C^a(\chi) = (2 - \cos^2\chi)\, H^a + (3\cos^2\chi - 1)\, I^a, \quad (16)$$

$$T^a(\tilde{\nu}_a) = \frac{1}{5hc}\cdot\frac{\mathrm{d}}{\mathrm{d}\tilde{\nu}_a}\ln\frac{\varkappa(\tilde{\nu}_a)}{\tilde{\nu}_a}, \quad (17)$$

$$U^a(\tilde{\nu}_a) = \frac{1}{10h^2c^2}\left[\left(\frac{\mathrm{d}}{\mathrm{d}\tilde{\nu}_a}\ln\frac{\varkappa(\tilde{\nu}_a)}{\tilde{\nu}_a}\right)^2 + \frac{\mathrm{d}^2}{\mathrm{d}\tilde{\nu}_a{}^2}\ln\frac{\varkappa(\tilde{\nu}_a)}{\tilde{\nu}_a}\right], \quad (18)$$

where $\varkappa(\tilde{\nu}_a)$ is the absorption coefficient at the wavenumber $\tilde{\nu}_a$.

$$D^a = 2\beta\,\mathrm{Re}\{\boldsymbol{m}_a\,\mathrm{m}_a{}'\,\boldsymbol{\mu}_g\} + |\,\mathrm{tr}\,\mathrm{m}_a{}'|^2, \quad (19)$$

$$E^a = \beta^2[3(\boldsymbol{m}_a\,\boldsymbol{\mu}_g)^2 - \mu_g{}^2] + \beta(3\,\boldsymbol{m}_a\,\boldsymbol{\alpha}_g\,\boldsymbol{m}_a - \mathrm{tr}\,\boldsymbol{\alpha}_g) + 6\beta\,\mathrm{Re}\{\boldsymbol{m}_a\,\boldsymbol{\mu}_g\cdot\mathrm{tr}\,\mathrm{m}_a{}' + \boldsymbol{\mu}_g\,\mathrm{m}_a{}'\,\boldsymbol{m}_a\} + 6\,|\,\mathrm{tr}\,\mathrm{m}_a{}'|^2, \quad (20)$$

$$F^a = \beta\,\boldsymbol{\mu}_g\,\Delta^a\boldsymbol{\mu} + \tfrac{1}{2}\,\mathrm{tr}\,\Delta^a\boldsymbol{\alpha} + 2\,\mathrm{Re}\{\boldsymbol{m}_a\,\mathrm{m}_a{}'\,\Delta^a\boldsymbol{\mu}\}, \quad (21)$$

$$G^a = \beta(\boldsymbol{m}_a\,\boldsymbol{\mu}_g)(\boldsymbol{m}_a\,\Delta^a\boldsymbol{\mu}) + \tfrac{1}{2}\,\boldsymbol{m}_a\,\Delta^a\boldsymbol{\alpha}\,\boldsymbol{m}_a + \mathrm{Re}\{\boldsymbol{m}_a\,\Delta^a\boldsymbol{\mu}\cdot\mathrm{tr}\,\mathrm{m}_a{}' + \Delta^a\boldsymbol{\mu}\,\mathrm{m}_a{}'\,\boldsymbol{m}_a\}, \quad (22)$$

$$H^a = |\,\Delta^a\boldsymbol{\mu}\,|^2, \quad (23)$$

$$I^a = |\,\boldsymbol{m}_a\,\Delta^a\boldsymbol{\mu}\,|^2. \quad (24)$$

In these terms it is

$$\beta = 1/kT \quad (25)$$

with the Boltzmann constant k and the temperature T. $L(\chi^0, \tilde{\nu}_a{}^0)$ is a constant, which arises from the influence of the external electric field on the absorption. $\boldsymbol{m}_e$ and $\boldsymbol{m}_a$ are unit vectors in the direction of the transition moments involved in the fluorescence and absorption process, respectively. $\mathrm{m}_e{}'$ and $\mathrm{m}_a{}'$ are tensors which describe the field dependence of the transition moment, as defined in [3].

$$\boldsymbol{\mu}_g = \mathrm{f}_e(1 - \mathrm{f}\,\boldsymbol{\alpha}_g{}^0)^{-1}\,\boldsymbol{\mu}_g{}^0, \quad (26)$$

$$\boldsymbol{\mu}_a = \mathrm{f}_e(1 - \mathrm{f}\,\boldsymbol{\alpha}_a{}^0)^{-1}\,\boldsymbol{\mu}_a{}^0, \quad (27)$$

$$\boldsymbol{\alpha}_g = \mathrm{f}_e{}^2(1 - \mathrm{f}\,\boldsymbol{\alpha}_g{}^0)^{-1}\,\boldsymbol{\alpha}_g{}^0, \quad (28)$$

$$\boldsymbol{\alpha}_a = \mathrm{f}_e{}^2(1 - \mathrm{f}\,\boldsymbol{\alpha}_a{}^0)^{-1}\,\boldsymbol{\alpha}_a{}^0, \quad (29)$$

$$\Delta^a\boldsymbol{\mu} = (1 - \mathrm{f}'\,\boldsymbol{\alpha}_a{}^{0\mathrm{FC}})^{-1}(1 - \mathrm{f}\,\boldsymbol{\alpha}_a{}^{0\mathrm{FC}})(1 - \mathrm{f}\,\boldsymbol{\alpha}_g{}^0)^{-1}\cdot(1 - \mathrm{f}'\,\boldsymbol{\alpha}_g{}^0)[\boldsymbol{\mu}_a{}^{\mathrm{FC}} - \boldsymbol{\mu}_g], \quad (30)$$

$$\Delta^e\boldsymbol{\mu} = (1 - \mathrm{f}\,\boldsymbol{\alpha}_a{}^0)^{-1}(1 - \mathrm{f}'\,\boldsymbol{\alpha}_a{}^0)(1 - \mathrm{f}'\,\boldsymbol{\alpha}_g{}^{0\mathrm{FC}})^{-1}\cdot(1 - \mathrm{f}\,\boldsymbol{\alpha}_g{}^{0\mathrm{FC}})[\boldsymbol{\mu}_a - \boldsymbol{\mu}_g{}^{\mathrm{FC}}], \quad (31)$$

$$\Delta^a\boldsymbol{\alpha} = \mathrm{f}_e{}^2(1 - \mathrm{f}'\,\boldsymbol{\alpha}_a{}^{0\mathrm{FC}})^{-1}(1 - \mathrm{f}\,\boldsymbol{\alpha}_g{}^0)^{-2}\cdot(1 - \mathrm{f}'\,\boldsymbol{\alpha}_g{}^0)(\boldsymbol{\alpha}_a{}^{0\mathrm{FC}} - \boldsymbol{\alpha}_g{}^0), \quad (32)$$

$$\Delta^e\boldsymbol{\alpha} = \mathrm{f}_e{}^2(1 - \mathrm{f}'\,\boldsymbol{\alpha}_g{}^{0\mathrm{FC}})^{-1}(1 - \mathrm{f}\,\boldsymbol{\alpha}_a{}^0)^{-2}\cdot(1 - \mathrm{f}'\,\boldsymbol{\alpha}_a{}^0)(\boldsymbol{\alpha}_a - \boldsymbol{\alpha}_g{}^{0\mathrm{FC}}) \quad (33)$$

with

$$\boldsymbol{\mu}_g{}^{\mathrm{FC}} = \mathrm{f}_e(1 - \mathrm{f}\,\boldsymbol{\alpha}_g{}^{0\mathrm{FC}})^{-1}\,\boldsymbol{\mu}_g{}^{0\mathrm{FC}}, \quad (34)$$

$$\boldsymbol{\mu}_a{}^{\mathrm{FC}} = \mathrm{f}_e(1 - \mathrm{f}\,\boldsymbol{\alpha}_a{}^{0\mathrm{FC}})^{-1}\,\boldsymbol{\mu}_a{}^{0\mathrm{FC}}, \quad (35)$$

$$\boldsymbol{\alpha}_g{}^{\mathrm{FC}} = \mathrm{f}_e{}^2(1 - \mathrm{f}\,\boldsymbol{\alpha}_g{}^{0\mathrm{FC}})^{-1}\,\boldsymbol{\alpha}_g{}^{0\mathrm{FC}}, \quad (36)$$

$$\boldsymbol{\alpha}_a{}^{\mathrm{FC}} = \mathrm{f}_e{}^2(1 - \mathrm{f}\,\boldsymbol{\alpha}_a{}^{0\mathrm{FC}})^{-1}\,\boldsymbol{\alpha}_a{}^{0\mathrm{FC}}. \quad (37)$$

In spherical approximation the cavity field factor $\mathbf{f}_e$ is given as

$$\mathbf{f}_e = \frac{3\varepsilon}{2\varepsilon+1}\mathbf{1} = f_e\mathbf{1}. \tag{38}$$

The reaction field tensors $\mathbf{f}$ and $\mathbf{f}'$ are given as:

$$\mathbf{f} = \frac{2}{a^3}\frac{1}{4\pi\varepsilon_0}\frac{\varepsilon-1}{2\varepsilon+1}\mathbf{1} = f\mathbf{1}, \tag{39}$$

$$\mathbf{f}' = \frac{2}{a^3}\frac{1}{4\pi\varepsilon_0}\frac{n^2-1}{2n^2+1}\mathbf{1} = f'\mathbf{1} \tag{40}$$

with the cavity radius a and the permittivity of the vacuum ε_0. ε is the dielectric constant and n the refractive number of the solvent.

In nonpolar solvents there is $\mathbf{f} = \mathbf{f}'$. Then Eqs. (30) to (33) get very simple:

$$\Delta^a\boldsymbol{\mu} = \boldsymbol{\mu}_a^{FC} - \boldsymbol{\mu}_g, \tag{41}$$

$$\Delta^e\boldsymbol{\mu} = \boldsymbol{\mu}_a - \boldsymbol{\mu}_g^{FC}, \tag{42}$$

$$\Delta^a\boldsymbol{\alpha} = \mathbf{f}_e^2(\mathbf{1} - \mathbf{f}\,\boldsymbol{\alpha}_a^{0FC})^{-1}(\mathbf{1} - \mathbf{f}\,\boldsymbol{\alpha}_g^{0})^{-1} \cdot (\boldsymbol{\alpha}_a^{0FC} - \boldsymbol{\alpha}_g^{0}), \tag{43}$$

$$\Delta^e\boldsymbol{\alpha} = \mathbf{f}_e^2(\mathbf{1} - \mathbf{f}\,\boldsymbol{\alpha}_a^{0})^{-1}(\mathbf{1} - \mathbf{f}\,\boldsymbol{\alpha}_g^{0FC})^{-1} \cdot (\boldsymbol{\alpha}_a^{0} - \boldsymbol{\alpha}_g^{0FC}). \tag{44}$$

The experimental setup for EOEM work is described in [26], a detailed study of EOAM apparatus is given in [27].

III. Results

III.1. Fluorescence Decay Times

With reference to [3] it is a strong demand that fluorescence decay times are much longer than reorientation times of the solvent and solute molecules. Otherwise the simple terms Eqs. (1) to (12) cannot be derived from EOEM experiments. So the fluorescence decay times in the solvents used have been determined by single photon counting methods. All solutions have not been de-aerated as the measuring cell for EOEM work cannot be sealed hermetically. Table 1 shows the results.

Table 1. Fluorescence decay times τ_f of ADMA solutions in heptane and dioxane, as determined at excitation wavenumbers $\tilde{\nu}_a$ and emission wavenumbers $\tilde{\nu}_e$ at 298 K.

Solvent	$\tilde{\nu}_a$ [10^5 m^{-1}]	$\tilde{\nu}_e$ [10^5 m^{-1}]	τ_f [10^{-9}s]
dioxane	25.2 ± 0.5	< 20.0	6.0 ± 0.1
heptane	26.2 ± 0.5	< 22.2	1.5 ± 0.2

The values found for τ_f are much larger than the reorientation relaxation times in these solvents, as is necessary for the evaluation of EOEM results. It must be emphasized that τ_f could be shown to be single exponential over more than three decades. This means that there is only one fluorescent species or state or a solvent dependent thermal equilibrium of two nearby electronic states in both solvents.

III.2. Low Temperature Fluorescence and Excitation Spectra of ADMA and Their Anisotropy

Figure 4 shows in a logarithmic scale the fluorescence and excitation spectra of ADMA and in a linear scale the anisotropy spectra of the fluorescence and excitation.

The anisotropy r is defined according to Jablonski [28]

$$r = \frac{I_\parallel - I_\perp}{I_\parallel + 2I_\perp}. \tag{45}$$

If the exciting light is linearly polarized, $I_\parallel$ denotes the component of the fluorescence light parallel to, $I_\perp$ that polarized perpendicular to the excitation polarization direction.

Decaline-methylcyclohexane (1:1) solutions have been glassy frozen and spectra have been taken around 110 K at 0.03 mol m^{-3} concentrations and at optical bandwidths of 200 cm^{-1}.

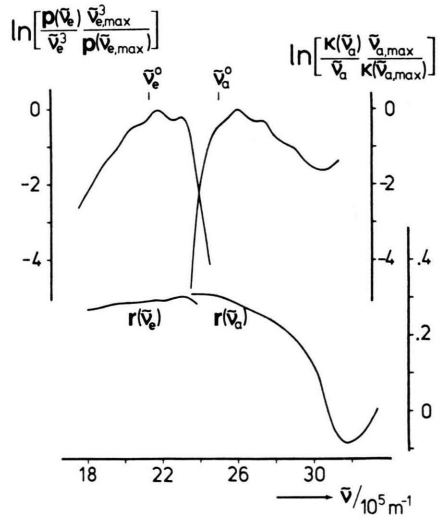

Fig. 4. Fluorescence and excitation spectra, degree of anisotropy $r(\tilde{\nu}_e)$ and $r(\tilde{\nu}_a)$ of the fluorescence (excitation: $\tilde{\nu}_a^0$) and excitation (emission: $\tilde{\nu}_e^0$) of ADMA in glassy frozen solutions in decaline-methylcyclohexane (1 : 1) at 110 K.

It could not be excluded quite certainly that the cell windows got dimmed to unvisibly small amounts, so the absolute values of the anisotropy could possibly be a little bit higher.

The excitation anisotropy is very similar to that of anthracene [29]. It must be emphasized that it is nearly constant at its maximum value at the long-wavelength shoulder of the excitation spectrum. Over the first vibrational bands it drops down a little, but it seems possible to do EOAM work not only in the longwavelength shoulder but in the first vibrational structure, too. The anisotropy spectrum of the fluorescence shows a very constant degree of anisotropy, so EOEM work should also give meaningful results. On the other hand these anisotropy spectra should not be overemphasized because they have been obtained at 110 K. EOAM and EOEM work is done at 298 K, thus the conditions could have changed very much. Especially, if the existence of an equilibrium of conformers is taken into account, the results of 110 K cannot be transformed to 298 K.

An important result is that the degree of anisotropy of the fluorescence at 298 K is smaller than 0.03, thus indicating that the lifetime of ADMA is much longer than all reorientation relaxation times involved. This is a further proof that the Eqs. (1) to (12) can be taken for the evaluation of EOEM data.

III.3. Results of EOEM work

Because of problems arising from dielectric breakdown in polar solvents, heptane as a nonpolar and dioxane as a pseudopolar solvent have been chosen. Both solvents have been freshly refluxed over NaK alloy for many hours before use. ADMA has been taken as supplied by Z. R. Grabowski. Fluorescing photoproducts that sometimes arose after some time of excitation, were eliminated by changing the solution.

Figures 5 and 6 show the fluorescence quantum spectra $p(\tilde{\nu}_e)/\tilde{\nu}_e^3$ of ADMA in heptane and dioxane and the primary spectrum $X(\varphi, \tilde{\nu}_e)$ of EOEM as defined in [3]. In Fig. 5 two independent spectra $X(\varphi, \tilde{\nu}_e)$ have been given to show the experimental error.

From these spectra $X(\varphi, \tilde{\nu}_e)$ the terms

$$D^e + 3L(\chi^0, \tilde{\nu}_a^0)$$

to I^e have been determined by a regression analysis. They are given together with single standard deviations as a measure for the statistical error in Table 2, together with the excitation wavenumber $\tilde{\nu}_a$ and the fluorescence spectral bandwidth $\delta\tilde{\nu}_e$.

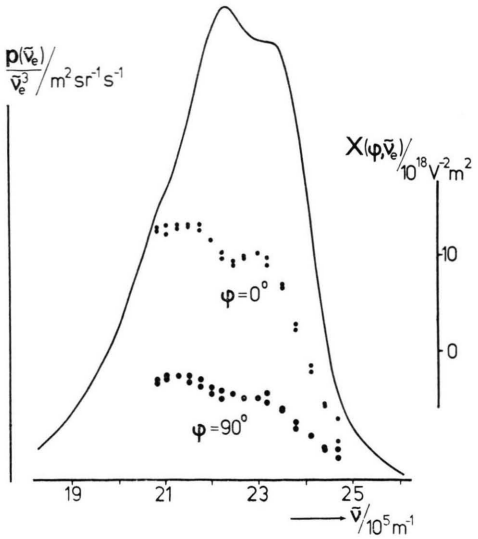

Fig. 5. ADMA in heptane at 298 K. Fluorescence spectrum $p(\tilde{\nu}_e)/\tilde{\nu}_e^3$ and two $X(\varphi, \tilde{\nu}_e)$ spectra, determined independently, as functions of φ and $\tilde{\nu}$.

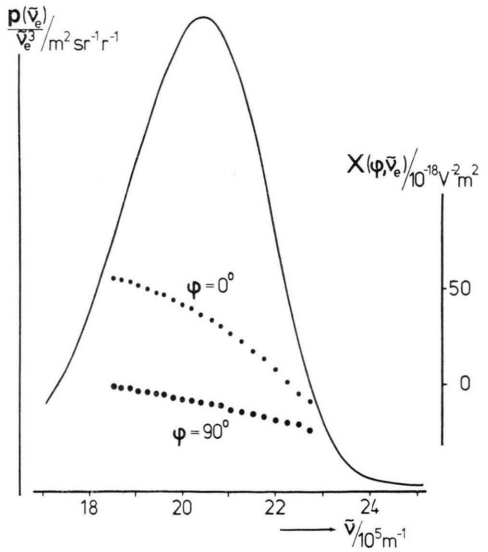

Fig. 6. ADMA in dioxane at 298 K. Fluorescence spectrum $p(\tilde{\nu}_e)/\tilde{\nu}_e^3$ and $X(\varphi, \tilde{\nu}_e)$ spectrum, as functions of φ and $\tilde{\nu}$.

In both cases the regression could be done over the entire fluorescence band, so showing a homogeneous fluorescence band. So a fluorescence of two conformers with different dipole moments or different spectra can nearly be excluded. On the other hand, the existence of two emitting nearby

Table 2. Results of EOEM work on ADMA at 298 K.

	Heptane	Dioxane
$D^e + 3L(\chi^0, \tilde{\nu}_a^0)$	70 ± 20	1980 ± 50
$(E^e - 2D^e)$ [10^{-20} m^2 V^{-2}]	13700 ± 150	45300 ± 200
F^e [10^{-40} CV^{-1} m^2]	2900 ± 100	10900 ± 200
G^e [10^{-40} CV^{-1} m^2]	2650 ± 100	10900 ± 200
H^e [10^{-60} C^2 m^2] / I^e [10^{-60} C^2 m^2]	could not be determined	
$\tilde{\nu}_a$ [10^5 m^{-1}]	$28 - 30$	$28 - 30$
$\delta\tilde{\nu}_e$ [10^5 m^{-1}]	0.5	0.4

electronic states in a thermal equilibrium cannot be excluded.

F^e and G^e have the same value within error. This indicates that $\boldsymbol{m}_e$, $\boldsymbol{\mu}_a$ and $\Delta^e\boldsymbol{\mu}$ are parallel, which could be argued, too, by symmetry. If explicit polarizability and transition polarizability terms are neglected which does not mean a large error with regard to the large dipole moments, the dipole moments listed in Table 3 can be determined.

Table 3. Dipole moments of ADMA as determined from EOEM.

	Determined from	Heptane	Dioxane
μ_a [10^{-30} Cm]	E^e	34.1 ± 0.2	61.9 ± 0.2
$\Delta^e\mu$ [10^{-30} Cm]	F^e	33.5 ± 1.4	72.5 ± 1.5
μ_g^{FC} [10^{-30} Cm]	E^e, $\frac{1}{2}(F^e + G^e)$	0.6 ± 1.4	(-10.6 ± 1.7)

μ_a in dioxane has nearly twice the value of μ_a in heptane. μ_g^{FC} is around zero. μ_g^{FC} in dioxane is not reliable because Eq. (42) is not correct in pseudo-polar dioxane.

III.4. Results of EOAM work on ADMA in the Longwavelength Shoulder

Electrooptical absorption measurements on ADMA have been performed at 298 K in heptane, dioxane and benzotrifluoride. The absorption spectra are shown in Figure 3. Figures 7 and 8 show a plot of $L(\chi, \tilde{\nu}_a)$ spectra over $U^a(\tilde{\nu}_a)$, in heptane and dioxane.

The longwavelength shoulder of the absorption spectra can be seen in these plots as the right part of the $L(\chi, \tilde{\nu}_a)$ spectrum decreasing from high to low $L(\chi, \tilde{\nu}_a)$ values with decreasing $U^a(\tilde{\nu}_a)$ values. The anthracene-like absorption is represented in the flat horizontal loops in the $L(\chi, \tilde{\nu}_a)$ spectrum. As the slope of the $L(\chi, \tilde{\nu}_a)$ spectrum is proportional

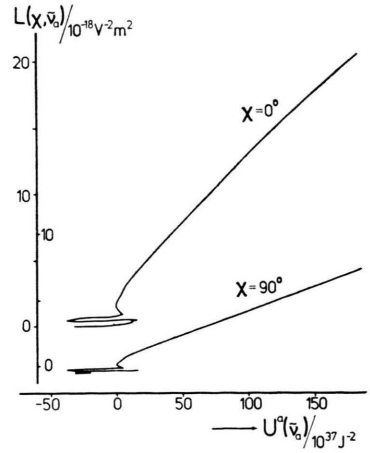

Fig. 7. ADMA in heptane at 298 K. $L(\chi, \tilde{\nu}_a)$ as a function of $U^a(\tilde{\nu}_a)$.

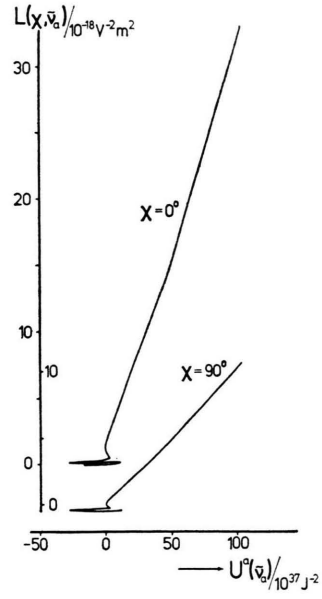

Fig. 8. ADMA in dioxane at 298 K. $L(\chi, \tilde{\nu}_a)$ as a function of $U^a(\tilde{\nu}_a)$.

to the square of the change of the dipole moment with excitation in a good approximation with ADMA, the longwavelength absorption shoulder must be interpreted as a transition to an excited FC-state, that has a large dipole moment, as it would be with Mataga's [7] „CT-state". As it was impossible to find any concentration dependence from 0.02 mol m^{-3} to 1 mol m^{-3}, this absorption cannot be attributed to a dimer absorption, whereas it could be assigned to as an absorption of a conformer of ADMA, with respect to the EOAM investigations.

Table 4. Results of EOAM on ADMA at 298 K in the longwavelength absorption shoulder.

	Heptane	Dioxane	Benzotrifluoride
D^a [10^{-20} V^{-2} m^2]	-70 ± 20	130 ± 20	190 ± 20
E^a [10^{-20} V^{-2} m^2]	550 ± 100	1700 ± 400	3100 ± 2000
F^a [10^{-40} CV^{-1} m^2]	480 ± 20		
G^a [10^{-40} CV^{-1} m^2]	430 ± 20		
H^a [10^{-60} C^2 m^2]	830 ± 15	3250 ± 250	3950 ± 300
I^a [10^{-60} C^2 m^2]	830 ± 15	3250 ± 250	3950 ± 300
$\frac{1}{2}(H^a + I^a)$ [10^{-60} C^2 m^2] *	785 ± 120	2700 ± 200	2970 ± 200
$\tilde{\nu}_a$ [10^5 m^{-1}]	23.4 – 25.2	22.3 ± 24.9	22.6–25.2
$\delta\tilde{\nu}_a$ [10^5 m^{-1}]	0.08	0.08	0.08

* See text.

The quantitative evaluation of data from EOAM is a little bit difficult because of the superposition of the two absorptions. In heptane a regression analysis could be performed, the results of which are given in Table 4. From $F^a = G^a \gg 0$ it follows with Eqs. (21), (22) that $\Delta^a\boldsymbol{\mu}$ has the same direction as $\boldsymbol{\mu}_g$, as had been supposed with respect to the good electron donor dimethylaniline.

For ADMA in dioxane and benzotrifluoride a complete regression according to Eqs. (13)—(18) could not be used, first because of the superposition of the absorption bands and second because $T^a(\tilde{\nu}_a)$ and $U^a(\tilde{\nu}_a)$ show very similar behaviour, that is, they are nearly linearly dependent. So in first approximation $B^a(\chi)$ was taken to be zero and then a regression analysis was performed. These results are shown in Table 4. With ${}^{I}\Delta^a\mu$ derived from H^a and I^a according to Eqs. (23), (24). $B^a(\chi)$ may be calculated taking $\mu_g \approx 7 \cdot 10^{-30}$ Cm. With this $B^a(\chi)$ a new $\frac{1}{2}(H^a + I^a)$ could be determined by recurrence. It is shown in Table 4, too. The spectral region where EOAM data have been derived is also shown, as is the spectral bandwidth $\delta\tilde{\nu}_a$ used in EOAM work.

The determination of μ_g, $\Delta^a\mu$ and μ_a^{FC} from the results Table 4 is done according to Eqs. (20)—(24) neglecting explicit polarizability terms and transition polarizabilities. μ_g is determined from E^a, ${}^{I}\Delta^a\mu$ from H^a and I^a and ${}^{II}\Delta^a\mu$ from $\frac{1}{2}(H^a + I^a)$ by recurrence. The results are shown in Table 5.

Taking $\mu_g = (7 \pm 2) \cdot 10^{-30}$ Cm, the dipole moment ${}^{I}\mu_a^{FC}$ of ADMA in heptane can be calculated from ${}^{I}\Delta^a\mu$ with Equation (41). Similarly ${}^{II}\mu_a^{FC}$ is determined from ${}^{II}\Delta^a\mu$. μ_a^{FC} in dioxane and benzotrifluoride determined by the same procedure must be considered to be an approximation, because Eq. (41) is not valid in these solvents. So these results are taken in brackets.

Table 5. Dipole moments of ADMA in heptane, dioxane and benzotrifluoride, determined from the longwavelength absorption shoulder.

		Heptane	Dioxane	Benzotrifluoride
μ_g	[10^{-30} Cm]	7 ± 0.6	12 ± 1.5	16.2 ± 6.5
${}^{I}\Delta^a\mu$	[10^{-30} Cm]	28.8 ± 0.3	57 ± 2.2	62.8 ± 2.4
μ_g	[10^{-30} Cm]	7 ± 2	7 ± 2	7 ± 2
${}^{I}\mu_a^{FC}$	[10^{-30} Cm]	35.8 ± 2.3	(64 ± 4.2)	(69.8 ± 4.4)
${}^{II}\Delta^a\mu$	[10^{-30} Cm]	28 ± 2	52 ± 2	54.5 ± 2
${}^{II}\mu_a^{FC}$	[10^{-30} Cm]	35 ± 4	(59 ± 4)	(61.5 ± 4)

III.5. Results of EOAM work on ADMA in the Anthracene-like Absorption

Although the degree of anisotropy of the excitation is not constant in the anthracene-like absorption, an evaluation of EOAM data could be performed by a complete regression according to Eqs. (13)—(18). The results are shown in Table 6, as well as the wavenumber interval taken for the evaluation and the spectral bandwidth used with EOAM.

The further evaluation of these data cannot be done similarly to the data from the longwavelength shoulder. Polarizability terms and transition polarizabilities cannot be neglected because of the small numbers in Table 6 compared with Table 4.

First it is assumed that $\mathrm{tr}\,\mathbf{m}_a' = 3\,\boldsymbol{m}_a \mathbf{m}_a' \boldsymbol{m}_a$, second $(3\,\boldsymbol{m}_a \boldsymbol{\alpha}_g \boldsymbol{m}_a - \mathrm{tr}\,\boldsymbol{\alpha}_g)$ is estimated to be $(8 \pm 8) \cdot 10^{-40}$ CV^{-1} m^2 from group polarizabilities. So from E^a the dipole moment μ_g can be calculated, and then from D^a the normalized transition polarizability $(\mathbf{m}_a')_{zz}$. From $H^a \approx I^a$ $\Delta^a\mu$ is determined and then from F^a and G^a with μ_g and $\Delta^a\mu$ the polarizabilities $\mathrm{tr}\Delta^a\boldsymbol{\alpha}$ and $(\Delta^a\boldsymbol{\alpha})_{zz}$, where $\boldsymbol{\mu}_g$ is taken to be antiparallel to $\Delta^a\boldsymbol{\mu}$. $\boldsymbol{\mu}_g \uparrow\downarrow \Delta^a\boldsymbol{\mu}$ must be

Table 6. Results of EOAM on ADMA in the anthracene-like absorption at 298 K.

	Heptane	Dioxane
D^a [10^{-20} V^{-2} m^2]	-50 ± 5	-90 ± 5
E^a [10^{-20} V^{-2} m^2]	550 ± 60	330 ± 20
F^a [10^{-40} CV^{-1} m^2]	-40 ± 30	-32 ± 7
G^a [10^{-40} CV^{-1} m^2]	-80 ± 20	-92 ± 10
H^a [10^{-60} C^2 m^2]	90 ± 20	60 ± 20
I^a [10^{-60} C^2 m^2]	105 ± 20	50 ± 10
$\tilde{\nu}_a$ [10^5 m^{-1}]	26.0 – 27.7	25.7 – 27.1
$\delta\tilde{\nu}_a$ [10^5 m^{-1}]	0.1	0.1

Table 7. Dipole moments of ADMA in heptane and dioxane determined from the anthracene-like absorption.

		Taken from	Heptane	Dioxane
μ_g	[10^{-30} Cm]	E^a, D^a	8.4 ± 0.5	8.4 ± 0.4
$(\mathbf{m}_a')_{zz}$	[10^{-10} m V^{-1}]	E^a, D^a	-1.2 ± 0.1	-2.2 ± 0.2
$\Delta^a\mu$	[10^{-30} Cm]	H^a, I^a	-9.9 ± 0.5	-7.4 ± 1
tr $\Delta^a\boldsymbol{\alpha}$	[10^{40} CV^{-1} m^2]	F^a	276 ± 100	172 ± 70
$(\Delta^a\boldsymbol{\alpha})_{zz}$	[10^{-40} CV^{-1} m^2]	G^a	198 ± 80	52 ± 50
μ_a^{FC}	[10^{-30} Cm]	μ_g, $\Delta^a\mu$	-1.5 ± 1.0	(1 ± 1.4)

deduced from the fact that F^a cannot be negative if $\boldsymbol{\mu}_g \uparrow\uparrow \Delta^a\boldsymbol{\mu}$, even if tr $\Delta\boldsymbol{\alpha} = -$ tr $\boldsymbol{\alpha}_g$. The results are shown in Table 7.

IV. Discussion

IV.1. Discussion of the Results of Electrooptical Investigations

From solvent shift measurements of the fluorescence and from EOEM it follows that the emitting state is a highly polar one. EOAM investigations showed that there is a transition to a highly polar excited FC state nearby the anthracene-like transition. In nonpolar heptane the dipole moment $\mu_a{}^{FC}$ from Table 5 may directly be compared with μ_a from Table 3. This is shown in Table 8.

The comparison of the dipole moment μ_a of the fluorescent state and the dipole moment $\mu_a{}^{FC}$ of the excited FC state corresponding to the longwavelength absorption shoulder supports the idea that the emitting state is the same as that reached by absorption in the longwavelength shoulder. A TICT formation [13] cannot be observed as it should show a large increase of the dipole moment μ_a. At the most a conformation that promotes TICT formation could be existent already in the ground state. An encouragement of the TICT formation with increasing solvent polarity cannot be observed. This is shown with all respect to the limited validity of Eq. (41) in dioxane by comparing μ_a Table 3 and $\mu_a{}^{FC}$ Table 5.

So a relaxation after excitation forming a new more polar species (like a TICT state) cannot be established.

μ_a	[10^{-30} Cm]	34.1 ± 0.2
$^I\mu_a^{FC}$	[10^{-30} Cm]	35.8 ± 2.3
$^{II}\mu_a^{FC}$	[10^{-30} Cm]	35 ± 4

Table 8. Comparison of μ_a and μ_a^{FC} of ADMA in heptane.

From Table 3 it can be seen that the dipole moment μ_a of ADMA in polar solvents is found to be larger than in nonpolar solvents. This fact is in good agreement with the solvent shift measurements of Mataga [7] and it has been taken as a fact advanced for a change of the structure in the excited state [12].

In the following it is shown that the solvent dependent dipole moment μ_a may be understood very well on the basis of a single conformer independent of solvent, in the ground and excited state.

The polarizabilities give rise to additional dipole moments induced by the reaction field. So $\mu_a{}^0$ can be assumed to be independent of solvent. From Eq. (27) follows with μ_a taken from Table 3 as determined in heptane and dioxane:

$$\frac{\mu_a{}^D}{\mu_a{}^H} = \frac{1 - f^H \alpha_a{}^0}{1 - f^D \alpha_a{}^0} = 1.815 \pm 0.017 . \qquad (46)$$

Heptane has been identified by upper right H, dioxane by D.

Similarly, from Eq. (31) the following quotient may be calculated with the data from Table 3:

$$\frac{{}^D\Delta^e\mu}{\mu_a{}^D - {}^D\mu_g{}^{FC}} = \frac{1 - f'^D \alpha_a{}^0}{1 - f^D \alpha_a{}^0} \cdot \frac{1 - f^D \alpha_g{}^0}{1 - f'^D \alpha_g{}^0} = 1.321 \pm 0.08 . \qquad (47)$$

${}^D\mu_g{}^{FC} = {}^D\mu_g = 7 \cdot 10^{-30}$ Cm has been taken parallel with the same direction as ${}^D\mu_a$.

From solvent shift measurements [30, 31] it is well known that the reaction field in dioxane is described by a dielectric constant ε of about 5 or 6.

So for further evaluation the following values are taken for ε and n:

$$\varepsilon_{\text{dioxane}} = 5 \quad (\text{or } 6) ,$$
$$\varepsilon_{\text{heptane}} = n^2_{\text{heptane}} = n^2_{\text{dioxane}} = 2 .$$

From this follows:

$$f'^D = f^H \qquad (48)$$

and

$$f^D/f'^D = f^D/f^H = 1.82 \text{ (or } 1.923) . \qquad (49)$$

Without further assumptions the terms given in Table 9 can be calculated from Eqs. (46) and (47).

With the values from Table 9 $\mu_a{}^0$ and $\mu_g{}^0$ are determined and given in Table 10.

ADMA has a dipole moment of around $19 \cdot 10^{-30}$ Cm in its first excited singlet state and about $4.5 \cdot 10^{-30}$ Cm in the ground state. The assumptions on ε do not influence the results very much.

Table 9. Terms $f\alpha$ and the quotient $\alpha_a{}^0/\alpha_g{}^0$ of ADMA.

Dioxane	5	6
f^D	0.644 ± 0.004	0.629
$f'^D \alpha_a{}^0 = f^H$	0.354 ± 0.002	0.327
$f^D \alpha_g{}^0$	0.453 ± 0.009	0.438
$f'^D \alpha_g{}^0 = f^H \alpha_g{}^0$	0.249 ± 0.005	0.228
$\alpha_a{}^0 : \alpha_g{}^0$	1.42 ± 0.03	1.43

Table 10. $\mu_a{}^0$ and $\mu_g{}^0$ of ADMA.

$\varepsilon_{\text{dioxane}}$	5	6
$\mu_a{}^0$ [10^{-30} Cm]	18.4 ± 0.1	19.1 ± 0.1
$\mu_g{}^0$ [10^{-30} Cm]	4.4 ± 1.3	4.5 ± 1.3

So it could be shown that the solvent dependence of μ_a of ADMA might be due to reaction field induced polarizabilities.

IV.2. Discussion of the Solvent Dependence of the Fluorescence of ADMA

In Part IV.1 it has been shown that implicit polarizabilities cannot be neglected if dipole moments of ADMA are determined by EOEM. Then it must be supposed that polarizabilities give rise to solvent shifts in addition to effects caused by permanent dipole moments. Then, Lippert's [32] and Mataga's [33] equations are no longer valid, but Liptay's equations [30] have to be taken, which take into account polarizabilities.

From Table 9 follows that it is $\alpha_a{}^0 - \alpha_g{}^0 < \alpha_g{}^0$.

So the last term in Eq. (26), Ref. [30] may be neglected. It is $\mu_a{}^0 \gg \mu_g{}^0$ and $f' \approx$ const. Hence, from Liptay [30, Eq. (26)] it follows

$$h\,c\,\tilde{\nu}_e = \text{const} - (\mu_a{}^0)^2 f\,(1 - f\,\alpha_a{}^0)^{-1}\,. \qquad (50)$$

From Table 9 it can be seen that $f\alpha_a{}^0$ is not small compared to 1. So a Mataga-Lippert plot of $\tilde{\nu}_e$ against f (or $f - \frac{1}{2}f'$) cannot show a straight line.

Defining $g = (\varepsilon - 1)/(2\varepsilon + 1)$, and taking $\varepsilon_{\text{dioxane}} = 5$, Eq. (50) may be rewritten using the values Table 9.

$$\tilde{\nu}_e = \text{const} - \frac{(\mu_a{}^0)^2}{hc}\,\frac{1}{a^3\,2\pi\,\varepsilon_0}\,F(g) \qquad (51)$$

with

$$F(g) = (g^{-1} - 1.77)^{-1}\,. \qquad (52)$$

A plot of $\tilde{\nu}_e$ against $F(g)$ Eq. (52) is shown in Fig. 9 using Mataga's [7] $\tilde{\nu}_e$, recalculated as mentioned above. This plot shows nearly a straight line.

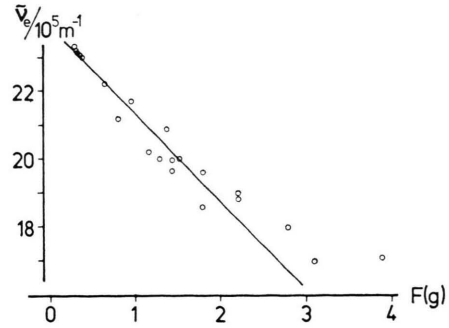

Fig. 9. A plot of the fluorescence wavenumber maximum $\tilde{\nu}_e$ of ADMA against $F(g)$ Eq. (52), according to Equation (51).

This procedure has been repeated, taking $\varepsilon_{\text{dioxane}} = 6$. This leads to the same Eq. (51) with

$$F(g) = (g^{-1} - 1.63)^{-1}\,. \qquad (53)$$

A plot of $\tilde{\nu}_e$ against $F(g)$ Eq. (53) according to Eq. (51) is shown in Figure 10. This plot shows a very good straight line.

As the slope of this line is very much smaller than in Fig. 1, a permanent dipole moment $\mu_a{}^0$ will result that is much smaller than that reported by Mataga.

The fact that a good straight line is obtained in fluorescence solvent shift measurements only, if polarizability terms are taken into account, must be looked upon as a proof that the interpretation of the results of electrooptical investigations on the basis of polarizability effects is correct. On the other hand, from these experiments no quantitative statements can be done with respect to the description of the internal field or even to an effective dielectric constant ε of dioxane. In order to do this, extensive electrooptical investigations in many really dipolar solvents must be performed.

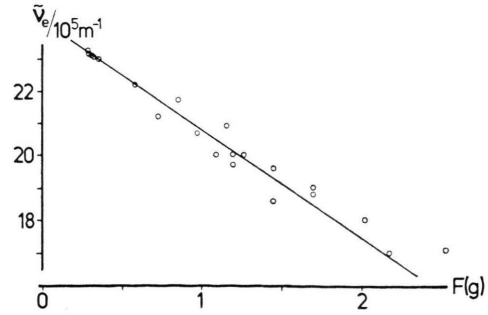

Fig. 10. A plot of the fluorescence wavenumber maximum $\tilde{\nu}_e$ of ADMA against $F(g)$ Equation (53), according to Equation (51).

Table 11. Results from the solvent dependence of the wavenumber of the fluorescence maximum of ADMA.

$\varepsilon_{\text{dioxane}}$		5	6
$(\mu_a{}^0)^2/a^3$	[10^{-30} C^2 m^{-1}]	4.6 ± 0.3	3.7 ± 0.3
$\mu_a{}^0$	[10^{-30} Cm]	18.4 ± 0.1	19.1 ± 0.1
a	[10^{-10} m]	4.2 ± 0.1	4.6 ± 0.1
$\alpha_g{}^0$	[10^{-40} CV^{-1} m^2]	51 ± 4	62 ± 4
$\alpha_a{}^0$	[10^{-40} CV^{-1} m^2]	72 ± 6	89 ± 7

Evaluation of the slope of the straight lines in Figs. 9 and 10 yields in a value for $(\mu_a{}^0)^2/a^3$ and with $\mu_a{}^0$ from Table 10, in a value for the cavity radius a, what seems to be a quite exact way of determining the cavity radius of a solute molecule. With this radius $\alpha_g{}^0$ and $\alpha_a{}^0$ can be determined. Table 11 shows these results.

$\alpha_g{}^0$ is in very good agreement with $\alpha_g{}^0$ from group polarizabilities, thus once more confirming the interpretation of the fluorescence behaviour of ADMA given in this paper.

The cavity radius determined experimentally and shown in Table 11 seems to be a little bit small as compared to $a = 5 \cdot 10^{-10}$ m, estimated from molecular dimensions.

But it must be taken into account that all considerations in this paper have been done in point dipole approximation. Quadrupole terms have not been taken into account. Furthermore, the assumption that the point dipole is in the center of the cavity, is a simplification with ADMA. All these unknown things are taken into account by the cavity radius as a parameter but as a parameter that could be determined experimentally.

IV.3. Discussion of the Solvent Dependence of the Rate Constant of the Fluorescence of ADMA

It is well known [6, 7, 34] that the rate constant $k_f{}^s$ of the fluorescence of ADMA solutions decreases with increasing solvent polarity. While Ref. [6] shows a monotonous decrease, Ref. [7] reports an abrupt decrease beyond $\varepsilon = 4$ to 5. This is interpreted as a hint to a solvent induced change of the structure of ADMA. In the following it is shown that this effect can also be understood, if polarizabilities are taken into account.

Using Liptay's [31] ideas concerning the solvent dependence of the intensity of electronic transitions, the solvent dependence of $k_f{}^s$ can be described by the following equation:

$$\sqrt{k_f{}^s} = \sqrt{k_f{}^0}\,[1 + (\mathbf{m}_e{}'^0)_{zz} f (1 - f\,\alpha_a{}^0)^{-1} \mu_a{}^0]\,. \quad (54)$$

Transition hyperpolarizabilities have been neglected. With $g = (\varepsilon - 1)/(2\varepsilon + 1)$, with $\varepsilon_{\text{dioxane}} = 6$ and with the data Table 9 it follows

$$\sqrt{k_f{}^s} = \sqrt{k_f{}^0}\left[1 + (\mathbf{m}_e{}'^0)_{zz} \frac{1}{a^3\, 2\pi\, \varepsilon_0} F(g)\, \mu_a{}^0\right]. \quad (55)$$

With $F(g)$ given in Equation (53).

A plot of $\sqrt{k_f{}^s}$ against $F(g)$ is shown in Figure 11. The values of Refs. [6] and [7] have been used as well as two values from Grabowski [34].

The first four points differ very much in Refs. [6] and [7] where $k_f{}^s$ has been taken with the quantum efficiency η of the fluorescence. $\eta = 0.3$ in hexane is taken from Ref. [7] and is in perfect agreement with [34]. The lower k_f use to be the more certain ones and as there are no comments on the discrepancy in Ref. [7] and as Grabowski's k_f value in *n* hexane is smaller than in [6], the larger values for k_f in the nonpolar or weakly polar solvents are neglected.

From the slope of the straight line in Fig. 11 $(\mathbf{m}_e{}'^0)_{zz}$ is determined to be:

$$(\mathbf{m}_e{}'^0)_{zz} = -\,6.9 \cdot 10^{-11}\,\text{V}^{-1}\,\text{m}\,.$$

With this value, D^e can be determined according to Equation (7). In heptane it follows

$$D^e = -\,210 \cdot 10^{-20}\,\text{V}^{-2}\,\text{m}^2\,.$$

This is a reasonable value but it cannot be determined experimentally, as $D^e + 3L(\chi^0, \tilde{\nu}_a{}^0)$ only is an experimental value. So a comparison with results from EOEM work is not possible.

But if we assume that the transition moment and its field dependence is the same for absorption and

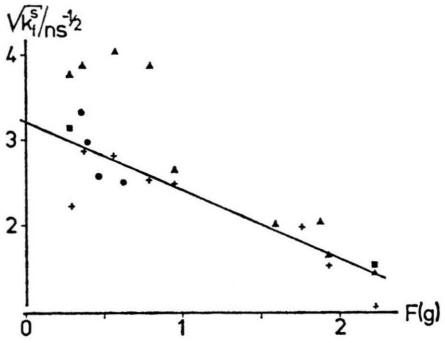

Fig. 11. A plot of $k_f{}^s$ against $F(g)$ Equation (53).
+++ according to [6];
▲▲▲ according to [7];
●●● according to [7] (DMF-MCH mixtures);
■■■ according to [34].

fluorescence, D^a may be calculated using Equation (19). In heptane D^a is found to be

$$D^a = -38 \cdot 10^{-20}\,V^{-2}\,m^2\,.$$

This value can be compared with D^a from Table 4. Table 4 shows $D^a = (-70 \pm 20) \cdot 10^{-20}\,V^{-2}\,m^2$.

This is in very good agreement if it is taken into consideration that D^a is very small compared to E^a and that the experimental error given for D^a is a single standard deviation only. Furthermore, it must be taken into account that there are additional errors from possible systematic errors suffering from the superposition of two electronic transitions in the absorption spectrum.

So the solvent dependence of k_f^s can also be understood consistently with the ideas described above, if terms like $(1 - f\alpha_a^0)$ are not neglected.

V. Electrooptical Investigations on Some Similar Molecules

Grabowski and his group [12, 13] not only have exploited spectroscopic and kinetic data on the fluorescence behaviour of ADMA but also on 4-(9-anthryl)-3,5-dimethyl-N,N-dimethylaniline (DMADMA) and 1-methyl-5-(9-anthryl)-indoline (MAI). This came from the idea that different conformers emit in different solvents [12]. So a steric hindrance should give more insight into the photophysics of these molecules.

A lot of samples of Grabowski's DMADMA and MAI have also been thoroughly investigated by electrooptical methods. These molecules show a quite distinct longwavelength shoulder in the absorption band similar to ADMA. The results of electrooptical measurements on this longwavelength shoulder in the absorption spectrum and on the entire fluorescence spectrum have been taken from similar considerations and computations as have been discussed in this paper for ADMA. The main results are given in Table 12.

Estimating $(3\,\boldsymbol{m}_a\boldsymbol{\alpha}_g\boldsymbol{m}_a - \mathrm{tr}\,\boldsymbol{\alpha}_g)$ to be $(8 \pm 8) \cdot 10^{-40}\,CV^{-1}\,m^2$, some dipole moments can be determined from electrooptical absorption measurements in the anthracene-like absorption, quite similar to those determined for ADMA in Chapter III.5. These dipole moments are given in Table 13 together with the values found for ADMA.

From these results and those of Table 12 μ_g is taken to be $(7 \pm 2) \cdot 10^{-30}$ Cm for all these molecules.

With this value and with ${}^{I}\Delta^a\mu$ or ${}^{II}\Delta^a\mu$ the FC state dipole moments $\mu_a{}^{FC}$ can be determined, as $\mu_g{}^{FC}$ can be from μ_a and $\Delta^e\mu$ according to Eq. (42) in heptane or cyclohexane.

The results are shown in Table 14.

The agreement between μ_a and $\mu_a{}^{FC}$ as well as between μ_g and $\mu_g{}^{FC}$ is good, taking into account the problems mentioned in Chapt. III.4 and considering the fact that $\mu_g{}^{FC}$ is given as a small difference of two large numbers. So the absorption

Table 12. Dipole moments of DMADMA and MAI determined from EOEM and from EOAM in the longwavelength shoulder of the absorption band. * in Cyclohexane.

		DMADAMA			MAI		
		Heptane	Dioxane	Fluoro-benzene	Heptane	Dioxane	Benzo-tri-fluoride
μ_a	[10^{-30} Cm]	45.6 ± 0.6 *	78.4 ± 0.2	83.2 ± 0.3	43.5 ± 0.3	72.7 ± 0.3	
$\Delta^e\mu$	[10^{-30} Cm]	52.8 ± 3 *	83.3 ± 2.6	85.2 ± 1.9	36.9 ± 2.1	75.3 ± 2	
μ_g	[10^{-30} Cm]				9.2 ± 2.5	0 ± 14.5	0 ± 13
${}^{I}\Delta^a\mu$	[10^{-30} Cm]	43.6 ± 2.2	80 ± 1.2	84.6 ± 1.1	46.4 ± 2.1	73.5 ± 1.3	74.8 ± 2
${}^{II}\Delta^a\mu$	[10^{-30} Cm]	40 ± 2	68 ± 2	74 ± 4	41 ± 4	65 ± 2	64 ± 2

Table 13. Dipole moments of ADMA, DMADMA and MAI determined by EOAM in the anthracene-like absorption.

		ADMA		DMADMA	MAI	
		Heptane	Dioxane	Heptane	Heptane	Dioxane
μ_g	[10^{-30} Cm]	8.4 ± 0.5	8.4 ± 0.4	6.3 ± 0.6	5.2 ± 0.3	7.6 ± 0.2
$\Delta^a\mu$	[10^{-30} Cm]	-9.9 ± 0.5	-7.4 ± 1	-5.5 ± 0.4	-4.7 ± 0.5	-5.2 ± 0.5
μ_a^{FC}	[10^{-30} Cm]	-1.5 ± 1	1 ± 1.4	0.8 ± 1	0.5 ± 0.8	2.4 ± 0.7

Table 14. Equilibrium state and FC state dipole moments of ADMA, DMADMA and MAI in nonpolar solvents.

		ADMA	DMADMA	MAI
μ_g	[10^{-30} Cm]	7 ± 2	7 ± 2	7 ± 2
μ_a	[10^{-30} Cm]	34.1 ± 0.2	45.6 ± 0.6	43.5 ± 0.3
μ_g^{FC}	[10^{-30} Cm]	0.6 ± 1.4	−7.2 ± 3.6	6.6 ± 2.4
$^{I}\mu_a^{FC}$	[10^{-30} Cm]	35.8 ± 2.3	50.6 ± 4.2	53.4 ± 4.1
$^{II}\mu_a^{FC}$	[10^{-30} Cm]	35 ± 4	47 ± 4	48 ± 4

process creates an excited FC state that has the same dipole moment as the emitting, relaxed state, in nonpolar solvents. That is, it is most possibly the same state with the same conformation. With DMADMA and MAI this state has a larger dipole moment μ_a than ADMA has.

This observation also holds for the pseudopolar dioxane and for benzotrifluoride or fluorobenzene.

Because of problems arising from the superposition of the longwavelength absorption shoulder and the anthracene-like absorption, the data determined from EOAM are not used for a quantitative determination of the dipole moments of the free molecules DMADMA and MAI. So a procedure can be followed quite similar to that given in Chapt. IV.1 for ADMA. Taking $\varepsilon_{dioxane}$ to be 5 as discussed above, the dipole moments given in Table 15 can be determined where μ_a^0 of ADMA has been taken from Table 11 for comparison.

Table 15. The dipole moments of the free molecules ADMA, DMADAMA and MAI

	ADMA	DMADMA	MAI
μ_a^0 [10^{-30} Cm]	18.4 ± 0.1	25.2 ± 0.5	24.3 ± 0.3
μ_g^0 [10^{-30} Cm]	4.4 ± 1.3	4.4 ± 1.3	4.4 ± 1.3

VI. Concluding Remarks

So all results of electrooptical measurements on ADMA, DMADMA and MAI can be understood by taking into account implicit polarizability effects, as induced by the solute point dipole via the reaction field. No conformational changes have to be assumed in order to explain these data, so forwarding the interpretation that there is really no conformational change after excitation nor a solvent dependent conformation in the solvents used in this paper.

In addition it seems to us that most of the results of experiments on these molecules as discussed in the literature can also be understood by solvent induced polarizability effects. So we believe that there is no experiment up to now that strikingly shows whether TICT formation and/or solvent induced polarizability effects stand for the fluorescence behaviour of these molecules. On the other hand we must see that the experimental results of this work can also be explained in the sense of Grabowski's TICT theory, as has been shown in Reference [35].

We thank Prof. Liptay for his interest and encouraging discussions, and we thank Prof. Grabowski and Mrs. Dr. Rotkiewicz for valuable discussions and that they have supplied us with the molecules discussed in this paper.

Financial support of this work by the Deutsche Forschungsgemeinschaft is gratefully acknowledged.

[1] W. Baumann, H. Deckers, K.-D. Loosen, and F. Petzke, Ber. Bunsenges. physik. Chem. **81**, 799 (1977).
[2] W. Baumann, J. Mol. Structure **47**, 237 (1978).
[3] W. Baumann and H. Deckers, Ber. Bunsenges. physik. Chem. **81**, 786 (1977).
[4] W. Liptay, in: Excited States, Vol. 1, p. 129, Academic Press, New York 1974.
[5] W. Liptay, Ber. Bunsenges. physik. Chem. **80**, 207 (1976).
[6] T. Okada, T. Fujita, M. Kubota, S. Masaki, N. Mataga, R. Ide, Y. Sakata, and S. Misumi, Chem. Phys. Lett. **14**, 563 (1972).
[7] T. Okada, T. Fujita, and N. Mataga, Z. physik. Chem. N.F. **101**, 57 (1976).
[8] R. Ide, Y. Sakata, S. Misumi, T. Okada, and N. Mataga, J. Chem. Soc., Chem. Comm. **1972**, 1009.
[9] N. Mataga, in: The Exciplex, eds. M. Gordon, W. R. Ware, p. 113, Academic Press, New York 1975.
[10] E. A. Chandross, in: The Exciplex, eds. M. Gordon, W. R. Ware, p. 187, Academic Press, New York 1975.
[11] N. Nakashima, N. Mataga, C. Yamanaka, R. Ide, and S. Misumi, Chem. Phys. Lett. **18**, 386 (1973).
[12] A. Siemiarczuk, Z. R. Grabowski, A. Krówczyński, M. Asher, and M. Ottolenghi, Chem. Phys. Lett. **51**, 315 (1977).
[13] Z. R. Grabowski, K. Rotkiewicz, W. Rubaszewska, and E. Kirkor-Kamińska, Acta physica Polon. **54**, 767 (1978).
[14] A. Siemiarczuk, Z. R. Grabowski, and A. Krówczyński, XIII Europ. Congress on Mol. Spectrosc., paper no. 263, Wroclaw 1977.
[15] H. E. Lessing and M. Reichert, Chem. Phys. Lett. **46**, 111 (1977).
[16] W. Rapp, H. H. Klingenberg, and H. E. Lessing, Ber. Bunsenges. physik. Chem. **75**, 883 (1971).
[17] H. Labhart, Helv. Chim. Acta **44**, 457 (1961).
[18] H. Labhart, Chimia **15**, 20 (1961).
[19] H. Labhart, Tetrahedron **19** (Suppl. 2), 223 (1962).
[20] W. Liptay and J. Czekalla, Z. Naturforsch. **15a**, 1072 (1960).

[21] W. Liptay and J. Czekalla, Ber. Bunsenges. physik. Chem. **65**, 721 (1961).
[22] W. Liptay, Z. Naturforsch. **20a**, 272 (1965).
[23] W. Liptay and G. Walz, Z. Naturforsch. **26a**, 2007 (1971).
[24] L. Onsager, J. Amer. Chem. Soc. **58**, 1486 (1936).
[25] Th. G. Scholte, Physica **15**, 437 (1949).
[26] H. Deckers and W. Baumann, Ber. Bunsenges. physik. Chem. **81**, 795 (1977).
[27] W. Baumann, Ber. Bunsenges. physik. Chem. **80**, 231 (1976).
[28] A. Jablonski, Bull. Acad. Polon. Sci., Sér. Sci. Math. Astron. Phys. **8**, 259 (1960).
[29] H. Zimmermann and N. Joop, Z. Elektrochem. **64**, 1215 (1960).
[30] W. Liptay, Z. Naturforsch. **20a**, 1441 (1965).
[31] W. Liptay, Z. Naturforsch. **21a**, 1606 (1966).
[32] E. Lippert, Z. Elektrochem. **61**, 962 (1957).
[33] N. Mataga, Y. Kaifu, and M. Koizumi, Bull. Chem. Soc. Japan **29**, 465 (1956).
[34] Z. R. Grabowski, private Communication.
[35] Z. R. Grabowski, K. Rotkiewicz, A. Siemiarczuk, D.J. Cowley, and W. Baumann, Nouveau J. Chim., **3**, 443 (1979).